5-12-2009

Effective dose from stray radiation for a patient receiving proton therapy for liver cancer

Phillip J. Taddei
University of Texas Health Science Center at Houston

Sunil Krishnan
University of Texas Health Science Center at Houston

Dragan Mirkovic
University of Texas Health Science Center at Houston

Pablo Yepes
Rice University

Wayne D. Newhauser
University of Texas Health Science Center at Houston

Recommended Citation

Taddei, P., Krishnan, S., Mirkovic, D., Yepes, P., & Newhauser, W. (2009). Effective dose from stray radiation for a patient receiving proton therapy for liver cancer. *AIP Conference Proceedings, 1099*, 445-449. https://doi.org/10.1063/1.3120070

Published in final edited form as:
AIP Conf Proc. 2009 March 10; 1099: 445–449. doi:10.1063/1.3120070.

Effective Dose from Stray Radiation for a Patient Receiving Proton Therapy for Liver Cancer

Phillip J Taddei[a], **Sunil Krishnan**[a], **Dragan Mirkovic**[a], **Pablo Yepes**[b], and **Wayne D Newhauser**[a,c]

[a]The University of Texas M. D. Anderson Cancer Center, 1515 Holcombe Blvd., Unit 94, Houston, TX 77030, USA

[b]Rice University, 6100 Main Street, MS 315, Houston, TX 77005, USA

Abstract

Because of its advantageous depth-dose relationship, proton radiotherapy is an emerging treatment modality for patients with liver cancer. Although the proton dose distribution conforms to the target, healthy tissues throughout the body receive low doses of stray radiation, particularly neutrons that originate in the treatment unit or in the patient. The aim of this study was to calculate the effective dose from stray radiation and estimate the corresponding risk of second cancer fatality for a patient receiving proton beam therapy for liver cancer. Effective dose from stray radiation was calculated using detailed Monte Carlo simulations of a double-scattering proton therapy treatment unit and a voxelized human phantom. The treatment plan and phantom were based on CT images of an actual adult patient diagnosed with primary hepatocellular carcinoma. For a prescribed dose of 60 Gy to the clinical target volume, the effective dose from stray radiation was 370 mSv; 61% of this dose was from neutrons originating outside of the patient while the remaining 39% was from neutrons originating within the patient. The excess lifetime risk of fatal second cancer corresponding to the total effective dose from stray radiation was 1.2%. The results of this study establish a baseline estimate of the stray radiation dose and corresponding risk for an adult patient undergoing proton radiotherapy for liver cancer and provide new evidence to corroborate the suitability of proton beam therapy for the treatment of liver tumors.

Keywords

proton radiotherapy; stray radiation; secondary neutrons; liver cancer; Monte Carlo; human phantoms

I. Introduction

Proton beam radiotherapy is an emerging treatment modality for patients with liver cancer because the unique physical characteristics of protons allow dose escalation to the clinical target volume (CTV) while sparing the nearby normal tissue. In photon or neutron therapy the maximum dose for each field is deposited near the surface of the patient, followed by a long exponential falloff of dose with depth along the beam path. In contrast, the maximum dose from a proton field is deposited near the end of a finite range, followed by a sharp and almost complete decrease in dose, virtually eliminating exit dose. This gives proton therapy a dosimetric advantage over photon radiotherapy in the sparing of nearby healthy tissues and organs. This is especially important for tumors that are near or within radiosensitive organs at risk for radiation carcinogenesis or toxicity. However, in the process of delivering a proton

[c]Corresponding Author: wnewhaus@mdanderson.org.

field that conforms to the CTV, stray radiation, mainly in the form of photons and neutrons, is produced, which can be detrimental to the patient and has no therapeutic benefit.[1-13] Exposure to neutrons, whether emanating from the treatment unit ("external neutrons") or inside the patient ("internal neutrons"), is of particular concern because neutrons are the predominant contributors to the effective dose from stray radiation. Furthermore, the relative biological effectiveness of neutrons for carcinogenesis is known to be high, although the exact value remains uncertain.[14] To our knowledge, the current study is the first to investigate exposure to neutrons for patients receiving proton therapy for liver cancer.

The rationale for treating liver cancer with protons is largely based on the need to spare as much of the healthy liver as possible. Radiotherapy of a partial liver volume is noninvasive, may slow the progression of the disease until resection or transplantation is viable, and is potentially curative. However, radiotherapy to the entire liver is usually toxic, limiting the dose that can be delivered and requiring the use of precise beams that can focus the radiation dose to a partial volume. Treatments with charged particle beams have been generally encouraging, and the limited clinical outcomes suggest that it may be possible to significantly improve tumor control rates.[15] Proton therapy for liver cancer has permitted dose escalation to the CTV without leading to dose-limiting toxicity, suggesting that this modality has potential as a curative treatment for liver cancer.[16] However, because of the risk for toxicity and second cancers—especially in the remaining liver volume, but also throughout the body—a better understanding of the stray neutron doses is needed.

The aim of this study, therefore, was to calculate the effective dose from stray radiation to a patient undergoing proton radiotherapy for liver cancer. To do this, we performed Monte Carlo simulations quantifying the radiation doses to various organs and tissues throughout the body. The geometric model used in the simulation consisted of a detailed double-scattering proton therapy treatment unit and a voxelized phantom based on computed tomography (CT) images of a patient diagnosed with liver cancer. We also estimated the risk of developing a second fatal cancer using risk coefficients from the literature and the calculated doses from the simulations.

II. Methods

II.A. Monte Carlo Model

In this study, we simulated a proton treatment for a large 59-year-old man diagnosed at our institution with primary hepatocellular carcinoma. The patient had undergone free-breathing CT imaging as part of treatment planning; using those same images, we created a proton treatment plan using a commercial treatment planning system (Eclipse Proton Planning; Varian Medical Systems, Inc., Palo Alto, CA).[17] The prescribed dose to 100% of the CTV (that is, the gross tumor volume plus margins) was 60 Gy. The plan was optimized for two proton fields, both having a posterior oblique beam configuration and passing through the treatment couch. One posterior oblique field (PO1) was delivered with a gantry rotation of 220°; a couch rotation of 45°; a proton beam energy of 225 MeV at the entrance of the treatment head, corresponding to a penetration range in the patient of 20.1 cm; a spread-out Bragg peak (SOBP) width of 14 cm; and a nominal gap of 23 cm between the distal component of the treatment unit, i.e., edge of the range compensator, and the proximal surface of the patient. The other posterior oblique field (PO2) was delivered with a gantry rotation of 135°; a couch rotation of -40°; a proton beam energy of 250 MeV at the entrance of the treatment head, corresponding to a penetration range in the patient of 25.0 cm; an SOBP width of 13 cm; and a nominal gap of 21 cm. Beam modifiers included a range-modulator wheel, scattering foil, range shifter, field-defining collimator, and range compensator.[17] The range compensator and field-defining collimator were carried within a snout that provided shielding and allowed for the shifting of the devices along the beam path. An intermediate size of the three available snouts was used for both

treatment fields (25-cm-diameter uncollimated field size, accommodating up to an 18 × 18 cm^2 collimated field). The field-defining collimator for both fields was 6 cm thick and made of brass.

Monte Carlo simulations were performed using the Monte Carlo N-Particle extended (MCNPX) code (version 2.6b)[18] with parallel computing methods. The suitability of the MCNPX code for simulating therapeutic absorbed dose distributions and secondary neutrons associated with proton therapy has been previously established.[2-4,17,19-26] The Monte Carlo model of the proton treatment unit included a proton source, the beam-modifying devices, the structural and housing components, and various static collimators.[8,17] A voxelized phantom representing the patient was based on the actual CT images for the patient, which included slices from the thighs to the top of the head. The Hounsfield unit value in each 4 mm × 4 mm × 5 mm voxel was converted to a mass density and a material composition.[27]

II.B. Dosimetric Calculations

The effective dose from neutrons, E, was calculated as

$$E=\sum_T (w_T H_T), \tag{1}$$

where w_T was the tissue (T) weighting factor and H_T was the equivalent dose to organs and tissues.[28] The w_T values were taken from the International Commission on Radiological Protection (ICRP) Publication 60.[29] H_T was calculated separately for internal neutrons and external neutrons for each treatment field as the product of the radiation weighting factor, w_R, and the mean absorbed dose for each organ or tissue, D_T, or

$$H_T=w_R D_T, \tag{2}$$

The w_R values for external neutrons were determined separately for each treatment field based on the calculated neutron spectral fluence incident upon the patient, following the recommendations in ICRP Publication 92.[28] The w_R values for internal neutrons were estimated based on the calculations of Zheng *et al.*[7] Using estimated values of w_R for internal neutrons introduced less than 10% uncertainty in E. D_T was calculated as the mass-weighted average of the absorbed dose of all voxels within the organ or tissue.

To calculate absorbed dose in each voxel per source particle, D_v/sp, (in Gy sp^{-1}), we performed separate simulations for therapeutic protons, external neutrons, and internal neutrons for each treatment field. For the external neutron simulations, neutrons and protons were tracked throughout the entire geometry except that all proton trajectories were terminated immediately upstream of the patient by a proton-stopping plane (imp:h=0,n>0), and D_v/sp was calculated throughout the patient using a type 3 mesh tally (keyword “total”). For the internal neutron simulations, neutrons were only tracked within the geometric model of the patient (outside patient, imp:h>0,n=0; inside patient, imp:h,n>0), i.e., external neutrons were not allowed to contribute to absorbed dose, and a more complex procedure was used for calculating D_v/sp from internal neutrons so that the contribution from recoil protons was included. For the therapeutic proton simulations, only protons were tracked throughout the model and the mass-averaged absorbed dose per source particle in the CTV, $D_{T=\mathrm{CTV}}$/sp, was calculated for each treatment beam. The reciprocal of $D_{T=\mathrm{CTV}}$/sp, that is, the number of protons per Gy in the CTV, was then used to normalize D_v/sp separately for each treatment field, resulting in E (in

mSv Gy^{-1}), H_T (in mSv Gy^{-1}), and D_T (in mGy Gy^{-1}). E and H_T values from individual treatment fields were combined to yield the corresponding quantities for the entire course of 60 Gy. Detailed methods for calculating these quantities have been described elsewhere.[30]

To achieve reasonable statistical uncertainties in D_T, 4×10^8, 4×10^8, and 2×10^8, source particle histories were tracked for the external neutron, internal neutron, and therapeutic proton simulations, respectively. Statistical uncertainties were based on the coefficients of variation reported by the MCNPX code at the 68% confidence interval. The uncertainties in the w_T and w_R values for internal neutrons were taken as zero.

III. Results

The values of E for each field are listed in Table 1. As shown, E for the entire treatment was 370 mSv (i.e., $E/D_{T=\mathrm{CTV}}$ was 6.17 mSv Gy^{-1}). The contribution of PO2, which had the higher initial proton energy, was 61% of the total E. The values of E from external and internal neutrons were 227 mSv (61% of total E) and 143 mSv (39% of total E), respectively, for the two-field treatment.

Table 2 lists the H_T values for the two posterior oblique fields for the 60-Gy treatment. H_T was larger for PO2 than for PO1 for each organ and tissue. Also listed are the sums of H_T for the two fields and the sums of $H_T w_T$, the proportion of the effective dose in each organ. The organs and tissues that received the greatest proportions of the effective dose were the lungs (18%), stomach (15%), liver (14%), red bone marrow (12%), colon (11%), and esophagus (8%). The distributions of absorbed dose from therapeutic protons and equivalent dose from neutrons throughout the patient are illustrated in Figure 1. The maximum mean equivalent dose to an organ or tissue from stray radiation was 1.03 Sv to the entire liver.

The calculated mean values of w_R for external neutrons were 8.892 ± 0.008 for PO1 and 8.944 ± 0.005 for PO2. The estimated value of w_R for internal neutrons was 9.6 for both fields. The total computing time for all simulations in this study was 4.4 cpu·years using parallel processing on 2.6-GHz, 64-bit microprocessors (AMD Opteron; Advanced Micro Devices, Inc., Sunnyvale, CA).

IV. Discussion

We calculated the effective dose from stray radiation, E, in a simulated treatment for a 59-year-old man receiving proton radiotherapy for liver cancer. The Monte Carlo calculations were based on a detailed model of a double-scattering proton therapy treatment unit and CT images from an actual patient for a complete 60-Gy proton treatment to the CTV. The total E was 370 mSv; 61% of E was from external neutrons, and 39% of E was from internal neutrons.

The value of the total E (370 mSv) was equivalent to the effective dose associated with approximately 20 whole-body CT scans. The National Council on Radiation Protection and Measurements has suggested that each Sv of low-dose and low-dose-rate exposure increases the fatal cancer risk by 3.2% for middle-aged men in general.[31] Thus, for a population of middle-aged men receiving the calculated total E, the corresponding excess attributable lifetime risk of a second cancer fatality would be approximately 1.2%. That is, about 12 of every 1000 middle-aged men treated in this way would die from second cancers caused by neutrons. Although this risk is small compared with the benefits of the radiotherapy, it is not negligible; methods to reduce the risk from neutrons emanating from the treatment unit are being explored.[30,32] Exposure to neutrons generated within the patient cannot be avoided. However, exposure to external neutrons may be mitigated through enhancements to the treatment unit.

In this study, we assumed a 60-Gy treatment to account for the possibility of future dose escalation. In the actual treatment plan, a dose of 60 cobalt Gray equivalent was prescribed, which corresponds to a 55-Gy proton treatment in current clinical practice.

Today liver cancer remains a deadly disease; improved treatment strategies are urgently needed. Proton radiotherapy provides a dosimetric advantage in that less healthy tissue in the liver is exposed, which introduces the possibility of escalating the dose to the diseased portion of the liver. Importantly, the results of this study clearly reveal the risks related to stray radiation are small compared to the benefits of proton radiotherapy. This is particularly relevant for hepatocellular carcinoma patients who choose proton radiotherapy as a bridge to liver transplantation—a scenario where treatment outcomes are excellent (up to 70% 5-year survival rates) and the likelihood of second malignancies after transplantation is higher than among patients undergoing non-transplant treatments (secondary to immunosuppression to prevent graft rejection). In summary, stray radiation should not be considered an obstacle to developing proton treatments for liver cancer.

Acknowledgments

The authors would like to acknowledge the assistance of John Carr, Jaques Bluett, and Daniel Jackson. We are indebted to Jonas Fontenot, Annelise Giebeler, Mark Harvey, Uwe Titt, Yuanshui Zheng, and Rui Zhang for helpful discussions and Kathryn B. Carnes for her assistance in preparing this manuscript. This work was supported in part by Northern Illinois University through a subcontract of Department of Defense contract W81XWH-08-1-0205.

References

1. Fontenot JD, Taddei P, Zheng Y, et al. Phys Med Biol 2008;53:1677. [PubMed: 18367796]
2. Polf JC, Newhauser WD. Phys Med Biol 2005;50(16):3859. [PubMed: 16077232]
3. Polf JC, Newhauser WD, Titt U. Radiat Prot Dosim 2005;115(1-4):154.
4. Tayama R, Fujita Y, Tadokoro M, et al. Nucl Instrum Meth A 2006;564:532.
5. Wroe A, Rosenfeld A, Schulte R. Med Phys 2007;34(9):3449. [PubMed: 17926946]
6. Yan X, Titt U, Koehler AM, et al. Nucl Instrum Meth B 2002;476:429.
7. Zheng Y, Fontenot J, Taddei P, et al. Phys Med Biol 2008;53(1):187. [PubMed: 18182696]
8. Zheng Y, Newhauser W, Fontenot J, et al. Phys Med Biol 2007;52(15):4481. [PubMed: 17634645]
9. Jiang H, Wang B, Xu XG, et al. Phys Med Biol 2005;50(18):4337. [PubMed: 16148397]
10. Agosteo S, Birattari C, Caravaggio M, et al. Radiother Oncol 1998;48(3):293. [PubMed: 9925249]
11. Schneider U, Agosteo S, Pedroni E, et al. Int J Radiat Oncol Biol Phys 2002;53(1):244. [PubMed: 12007965]
12. Zacharatou Jarlskog C, Lee C, Bolch WE, et al. Phys Med Biol 2008;53(3):693. [PubMed: 18199910]
13. Taddei PJ, Mirkovic D, Fontenot JD, et al. Phys Med Biol. in press.
14. Brenner DJ, Hall EJ. Radiother Oncol 2008;86(2):165. [PubMed: 18192046]
15. Hawkins MA, Dawson LA. Cancer 2006;106(8):1653. [PubMed: 16541431]
16. Krishnan S, Dawson LA, Seong J, et al. Ann Surg Oncol 2008;15(4):1015. [PubMed: 18236114]
17. Newhauser W, Fontenot J, Zheng Y, et al. Phys Med Biol 2007;52(15):4569. [PubMed: 17634651]
18. Pelowitz, DB., editor. MCNPXTM User's Manual, Version 2.5.0. Los Alamos, New Mexico: Los Alamos National Laboratory; 2005.
19. Herault J, Iborra N, Serrano B, et al. Med Phys 2005;32(4):910. [PubMed: 15895573]
20. Herault J, Iborra N, Serrano B, et al. Med Phys 2007;34(2):680. [PubMed: 17388186]
21. Fontenot JD, Newhauser WD, Titt U. Radiat Prot Dosim 2005;116(1-4 Pt 2):211.
22. Koch N, Newhauser W. Radiat Prot Dosim 2005;115(1-4):159.
23. Newhauser W, Koch N, Hummel S, et al. Phys Med Biol 2005;50(22):5229. [PubMed: 16264250]
24. Newhauser WD, Koch NC, Fontenot JD, et al. Phys Med Biol 2007;52(13):3979. [PubMed: 17664589]

25. Koch N, Newhauser WD, Titt U, et al. Phys Med Biol 2008;53:1581. [PubMed: 18367789]
26. Titt U, Sahoo N, Ding X, et al. Phys Med Biol 2008;53(16):4455. [PubMed: 18670050]
27. Newhauser WD, Giebeler A, Langen KM, et al. Phys Med Biol 2008;53(9):2327. [PubMed: 18421122]
28. Ann ICRP. Vol. 33. New York: Pergamon; 2003. ICRP Publication 92.
29. Ann ICRP. Vol. 21. New York: Pergamon Press; 1991. ICRP Publication 60.
30. Taddei PJ, Fontenot JD, Zheng Y, et al. Phys Med Biol 2008;53:2131. [PubMed: 18369278]
31. NCRP. Uncertainties in Fatal Cancer Risk Estimates Used in Radiation Protection. Bethesda, Maryland: National Council on Radiation Protection and Measurements; 1997.
32. Taddei PJ, Mrkovic D, Fontenot JD, et al. Nucl Technol. in press.

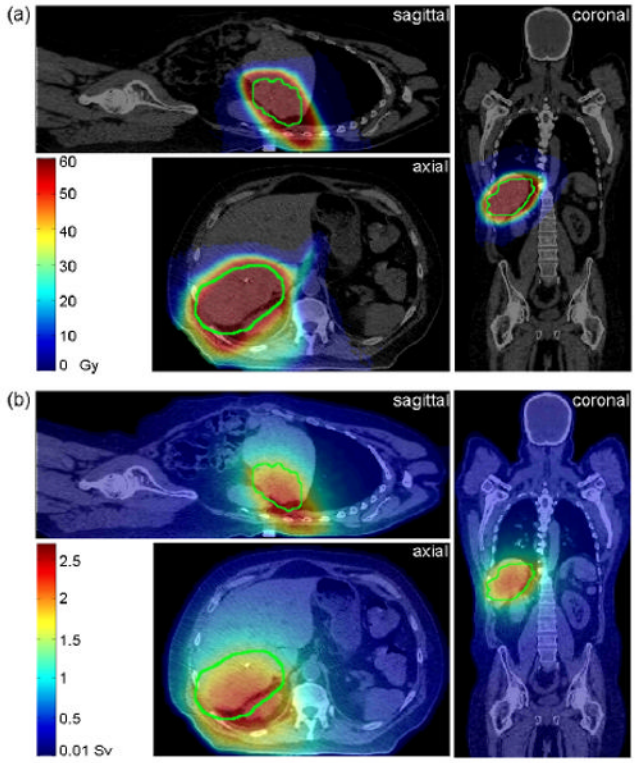

FIGURE 1.
Absorbed dose from therapeutic protons in Gy (a) and equivalent dose from neutrons in Sv (b) shown in planes that intersect the isocenter. The CTV is delineated in bright green.

TABLE 1

Effective dose from neutrons, *E*, for posterior oblique proton treatment fields PO1 and PO2. The effective dose is further broken down into contributions from external and internal neutrons.

	***E* (mSv)**		
Field	**External**	**Internal**	**Total**
PO1	81	63	144
PO2	146	80	226
Total	*227*	*143*	*370*

TABLE 2

Equivalent dose in organs and tissues from neutrons, H_T, for a 60-Gy treatment. H_T is separated into contributions from treatment fields PO1 and PO2. Statistical uncertainty, $\sigma(H_T)$, is listed in terms of percentage of H_T. Also listed is the proportion of effective dose from neutrons, $H_T w_T$, in each organ or tissue. w_T is the tissue weighting factor for effective dose.

Organ or tissue	w_T	H_T(PO1) (mSv)	H_T(PO2) (mSv)	H_T (mSv)	$\sigma(H_T)/H_T$	$H_T w_T$ (mSv)
Gonads	0.20	41	61	102	2.90%	20.3
Red bone marrow	0.12	131	255	385	0.16%	46.2
Colon	0.12	143	191	333	0.20%	40.0
Lungs	0.12	199	368	568	0.45%	68.1
Stomach	0.12	190	257	447	0.41%	53.6
Bladder	0.05	66	98	163	1.63%	8.2
Breasts	0.05	100	165	265	3.02%	13.3
Liver	0.05	458	567	1025	0.13%	51.3
Esophagus	0.05	220	394	614	0.79%	30.7
Thyroid	0.05	90	173	263	1.65%	13.1
Skin	0.01	138	225	363	0.04%	3.6
Bone surface	0.01	116	219	335	0.09%	3.4
Remainder	0.05	137	224	361	0.04%	18.0